ChemSusChem

Research Article
doi.org/10.1002/cssc.202200418

Chemistry Europe
European Chemical Societies Publishing

www.chemsuschem.org

Challenges of Green Production of 2,5-Furandicarboxylic Acid from Bio-Derived 5-Hydroxymethylfurfural: Overcoming Deactivation by Concomitant Amino Acids

Dominik Neukum,[a] Lorena Baumgarten,[a] Dominik Wüst,[c] Bidyut Bikash Sarma,[a] Erisa Saraçi,[a, b] Andrea Kruse,[c] and Jan-Dierk Grunwaldt*[a, b]

The oxidation of 5-hydroxymethylfurfural (HMF) to 2,5-furandicarboxylic acid (FDCA) is highly attractive as FDCA is considered as substitute for the petrochemically derived terephthalic acid. There are only few reports on the direct use of unrefined HMF solutions from biomass resources and the influence of remaining constituents on the catalytic processes. In this work, the oxidation of HMF in a solution as obtained from hydrolysis and dehydration of saccharides in chicory roots was investigated without intermediate purification steps. The amount of base added to the solution was critical to increase the FDCA yield. Catalyst deactivation occurred and was attributed to poisoning by amino acids from the bio-source. A strong influence of amino acids on the catalytic activity was found for all supported Au, Pt, Pd, and Ru catalysts. A supported AuPd(2:1)/C alloy catalyst exhibited both superior catalytic activity and higher stability against deactivation by the critical amino acids.

Introduction

The production of bio-based building blocks as alternative to fossil-based resources has recently received a significant interest from industry as well as academia. One important platform molecule and promising substitute for the fossil-derived terephthalic acid in the production of renewable polyesters is 2,5-furandicarboxylic acid (FDCA), as identified by the US Department of Energy in 2004.[1] This potential building block can be obtained via selective oxidation of biomass-derived 5-hydroxymethylfurfural (HMF). Therefore, different approaches like heterogeneous, homogeneous, bio-, and electro-catalytic oxidation, as well as procedures without any catalyst, are presently discussed for industrial applications.[2] The easy separation and reusability of a solid catalyst makes this route more attractive than others, would contribute to a green conversion of HMF, and is very promising for industrial implementation.[2b] As introduced earlier,[8a] the oxidation of HMF starts with the oxidation of either the hydroxymethyl or aldehyde function (Scheme 1) to 5-hydroxymethylfuran-2-carboxylic acid (HFCA) or 2,5-diformylfuran (DFF), respectively. These intermediates are then further oxidized to 5-formyl-2-furancarboxylic acid (FFCA) and FDCA (details on the reaction mechanism reported by Davis et al.[3] and Ardemani et al.,[4] see the Supporting information).

HMF can be synthesized from different bio-based sources like monosaccharides (glucose and fructose) or polymers (e.g., cellulose and inulin).[5] Nevertheless, monosaccharides are mainly extracted from plants also used for food production. Therefore, using inedible plant parts, which are not competing with the food chain (e.g., agricultural waste material) is preferable and will lead to a cheaper and more sustainable process.[5a] Chicory root, which contains a high fraction of inulin, is a promising example.[6] Although one of the main criteria for the extensive research on green FDCA synthesis is the use of abundant and renewable biomass resources, investigations on the oxidation of HMF from real biomass to FDCA have hardly been reported in the literature. Thus, the influence of impurities in the feedstock from biomass on the catalytic system is often

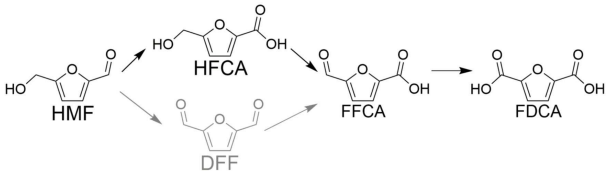

Scheme 1. Oxidation of HMF to FDCA (DFF formation not observed in this work).

[a] D. Neukum, L. Baumgarten, Dr. B. B. Sarma, Dr. E. Saraçi, Prof. Dr. J.-D. Grunwaldt
Institute of Catalysis Research and Technology,
Karlsruhe Institute of Technology
Hermann-von-Helmholtz-Platz 1,
76344 Eggenstein-Leopoldshafen (Germany)
E-mail: grunwaldt@kit.edu
[b] Dr. E. Saraçi, Prof. Dr. J.-D. Grunwaldt
Institute for Chemical Technology and Polymer Chemistry,
Karlsruhe Institute of Technology
Engesserstraße 20, 76131 Karlsruhe (Germany)
[c] D. Wüst, Prof. Dr. A. Kruse
Institute of Agricultural Engineering,
University of Hohenheim
Garbenstraße 9,70593 Stuttgart (Germany)

Supporting information for this article is available on the WWW under https://doi.org/10.1002/cssc.202200418

This publication is part of a collection of invited contributions focusing on "Green Conversion of HMF". Please visit chemsuschem.org/collections to view all contributions.

not considered.[7] Naim et al.[7] observed a major decrease in the FDCA yield using an Au/ZrO_2 catalyst in presence of 0.25 equiv. of levulinic and formic acid in the solution, which are among the main side products of HMF synthesis from fructose. This shows the necessity to investigate the influence of such feedstock ingredients. Moreover, purification steps in the production of highly pure HMF are a major reason for the high costs of the process chain due to multiple reaction and separation steps needed.

New catalyst formulations are an essential tool for overcoming deactivation issues and increasing the FDCA yield. Various compositions for heterogeneous catalysts have been reported over the last years. These catalysts predominantly consist of noble metals such as Au,[3a,8] Pt,[8c,9] Pd,[8c,10] Ru,[11] as well as alloys[12] of these metals as active component. For example, FDCA was obtained in a yield of >99% with gold supported on hydrotalcite without the addition of any base to the solution.[8e] The elimination of a base makes this approach more sustainable, but serious concerns about the stability of hydrotalcite in water make it not so viable for large-scale application.[4] On the other hand, the utilization of Pt or Ru as active metals allows for the use of weaker bases. Ait Rass et al.[9b] reported a procedure with a yield of 69% FDCA with a Pt/C catalyst at 100 °C, 40 bar of synthetic air, and 2 equiv. of Na_2CO_3. The yield could even be improved to 98% when adding 1% Bi to the catalyst. Yi et al.[11a] investigated the activity of Ru/C catalyst in the presence of different bases and achieved a FDCA yield of 95% with $CaCO_3$ as base. In an alternative approach, Gui et al.[12c] achieved a yield of >99% FDCA with an AuPd(*n*/*n* 1:1) alloy-based catalyst supported on zinc hydroxycarbonate by using $NaHCO_3$ as weak base. The use of AuPd alloy-based catalysts also allows for base-free conditions, as shown by Bonincontro et al.[12b] with AuPd(6:4) alloy supported on nanosized NiO. The authors attributed the activity to synergistic effects of Au, Pd, and the support material. Furthermore, improved activity and stability of Au-rich alloys AuPd(8:2) supported on activated carbon, which showed quantitative conversion to FDCA after 2 h, was presented by Villa et al.[12a] A change in the electronic properties of the alloy was emphasized as the reason for the catalytic activity.

In this work, the use of a raw HMF solution obtained by hydrothermal dehydration of fructose-rich extract has been studied for the oxidation to FDCA. Therefore, forced chicory roots, which are an agricultural by-product, were considered as attractive and sustainable feedstock. A greener process can be achieved by bridging HMF synthesis from bio-resources and its oxidation to FDCA. Due to the broad scope of carbon as substrate being used for supporting different noble metals[8c,9b,11a,12a] we chose carbon black Vulcan as support material for most of the catalysts. The aim was to systematically study the influence of selected amino acids on the stability and activity of typical noble metals used for the heterogeneously catalyzed oxidation of HMF to FDCA. For this purpose, Au, Pt, Pd, and Ru catalysts supported on carbon black were prepared and tested in the oxidation of HMF in presence of varying concentrations of amino acids. Surprisingly, we discovered a significant influence of amino acids from the bio-source on the catalytic activity and stability. Finally, Au and Pd alloys in different ratios were investigated with the aim to further improve the activity and stability of the catalysts.

Results and Discussion

Catalyst characterization

The noble metal loading on the support was determined by inductively coupled plasma optical emission spectrometry (ICP-OES) and the specific surface area was measured by the Brunauer-Emmett-Teller (BET) method. The noble metal loading for all catalysts is between 1.5 and 2 wt% making them well comparable for the catalytic tests. Two measurements were performed with ICP-OES for each sample and the results are similar (±0.03 wt%), showing a good homogeneity of the catalysts. Moreover, the ratio of Au to Pd in the bimetallic catalysts is close to the intended ratio. The specific surface area of all catalysts is in a comparable range of around 200 to 220 $m^2 g^{-1}$ (for details see Table S3), showing only small decrease upon the noble metal introduction compared to the pure carbon support with a surface area of 241 $m^2 g^{-1}$. Impregnation (ip) method for Pt/C results in a further decrease of the specific surface area due to the enhanced temperature applied during reduction.

Powder X-ray diffraction (XRD) patterns (Figure 1) showed reflections of Au and Pd in the monometallic catalysts, while no

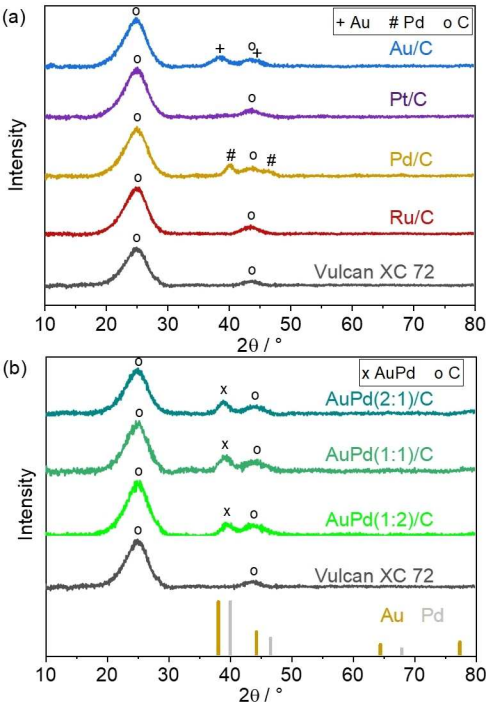

Figure 1. Powder XRD patterns of (a) Au/C, Pt/C, Pd/C, Ru/C, and carbon black support, and (b) AuPd(2:1)/C, AuPd(1:1)/C, AuPd(1:2)/C, and carbon black support. The Au and Pd reflections are shown from ICSD reference (ICSD reference code: Au – 00-004-0784, Pd – 00-046-1043) crystallographic data.

reflections of Pt and Ru particles (Pt: 39.8° 2θ; Ru: 43.5° 2θ) are visible. The reason for the latter is the presence of very small and highly dispersed nanoparticles with a size below the detection limit of XRD.[8b,13] Indeed, the mean particle diameter was determined as 1.5 ± 0.4 nm for Pt/C and 1.1 ± 0.2 nm for Ru/C by transmission electron microscopy (TEM) (see Figures S12 and S14). In contrast, the mean particle diameter for Au/C and Pd//C was 3.3 ± 1.2 nm and 4.2 ± 1.8 nm, respectively (see Figures S11 and S13). For the bimetallic catalysts, reflections of the noble metal particles are between 2θ = 38.2 and 40.1° indicating the formation of an alloyed face-centered cubic (fcc) phase of Au and Pd (Figure 1b).[13] A nearly linear shift of the reflection from 39.1 to 39.5° with increasing Pd fraction was observed. The reflections of the carbon support at 24.9 and 43.9° are broad due to its mostly amorphous nature. For Au/ZrO_2, no reflections of metallic Au were detected as already reported (see Figure S2).[8b]

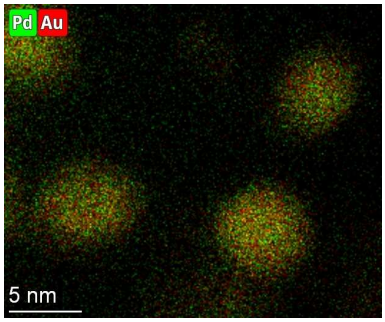

Figure 2. EDX-mapping of AuPd(2:1)/C (green: Pd; red: Au).

The catalysts were further characterized by TEM, and the mean diameters were obtained by averaging over 150 particles, which were found to be in the range between 3.5 to 4.1 nm for bimetallic catalysts (see Figures S15–S17). In addition, energy-dispersive X-ray spectroscopy (EDX) mapping of AuPd(2:1)/C showed a homogeneous distribution of Au and Pd over the bimetallic nanoparticle (Figure 2). Thereby, no indication of the formation of segregated phases of Au and Pd (e.g., in a core-shell like structure)[14] were found. This supports the conclusion from XRD that one dominant alloyed phase is formed.

The small reflections of bimetallic catalysts in the XRD pattern, due to small particles, draw vague conclusions about the AuPd alloy formation. Therefore, X-ray absorption spectroscopy (XAS) measurements of the bimetallic catalysts at the Au L_3- and Pd K-edge were performed to determine the oxidation state of Au and Pd, as well as to confirm the alloy formation. The X-ray absorption near edge structure (XANES) normalized spectra, which are the fingerprint of the oxidation state, of AuPd samples at the Au L_3-edge show similarities of the catalysts with the AuPd(1:1) foil in the white line features indicating alloy formation (Figure 3a). Similarly, spectra meas-

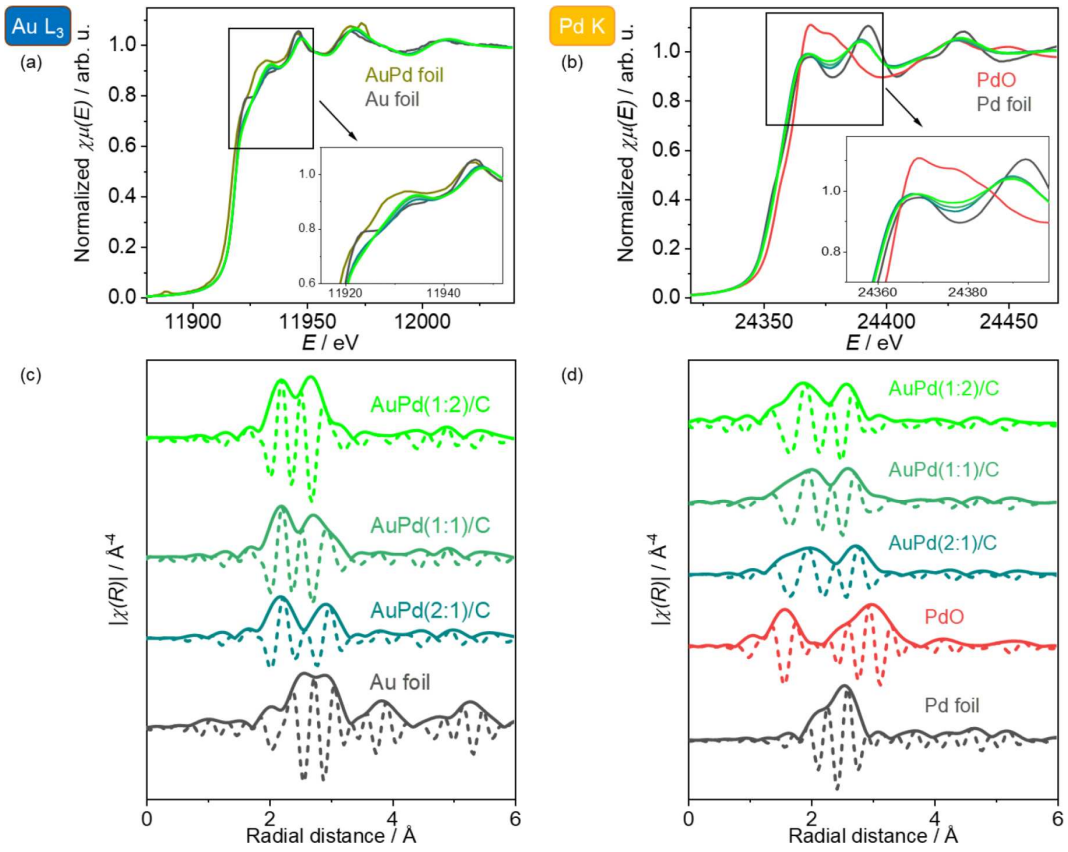

Figure 3. Normalized XANES spectra of the catalysts at (a) Au L_3-edge and (b) Pd K-edge, and Fourier-transformed (FT) k^3-weighted EXAFS spectra of bimetallic AuPd/C catalysts at (c) Au L_3-edge and (d) Pd K-edge. Standard reference oxide and foil (AuPd reference from ESRF) are shown.

ured at Pd K-edge for the three bimetallic catalysts, Pd foil, and PdO showed different features suggesting that Pd might be in an alloy state since the catalyst features are significantly different from Pd–Pd interaction and especially Pd–O interaction (Figure 3b). There are changes in the near edge structure at both Au L_3-edge and Pd K-edge, depending on the ratio of Au/Pd in the bimetallic samples, which might be attributed to an interaction by electron transfer between Au and Pd as previously observed for AuAg alloys.[15]

Fitting of the Fourier-transformed extended X-ray absorption fine structure (EXAFS) spectra (Figure 3a) at Au L_3-edge with Artemis software reveal scattering by Au–Au as well as Au–Pd in the first shell in all alloyed catalysts (for details see Table S4 and Figure S5).[16] A radial distance of about 2.8 Å (phase-uncorrected) is expected for AuPd alloys for Au–Au as well as Au–Pd scattering, which was obtained as result of the fitting, proving the successful alloy formation.[17] The two peaks at around 2.2 and 2.7–2.9 Å are both assigned to first shell metal-metal contribution. This peak is split into two due to an interference of Au–Au and Au–Pd backscattering because of a different phase shift and amplitude.[17a,c] While ICP-OES revealed Au/Pd ratios close to the intended ratio, fitting of EXAFS spectra showed Au-enriched phases for all alloys. Note that ICP-OES gives Au/Pd ratio in wt% while XAS refers to the molar ratio of Au/Pd. A reason for this observation might be a compositional gradient in the alloy with a Pd enriched shell due to lower CN for Au–Pd scattering compared to Au–Au scattering.[15] In addition, Fourier-transformed EXAFS spectra measured at Pd K-edge suggest the presence of non-reduced $PdCl_2$ from the precursor on the catalyst surface. However, no reflections of $PdCl_2$ could be found in XRD indicating the presence of only minor amounts of $PdCl_2$ in the catalyst.

Oxidation of chicory root-derived HMF solution

To examine the applicability of bio-based HMF solutions for the catalytic oxidation with noble metal-based catalysts, we tested the oxidation of HMF in a chicory root-derived solution (HMF Chic; 0.004 M HMF) with an Au/ZrO_2 catalyst. Therefore, we used reaction conditions optimized in our previous study (125 °C, 30 bar pressure of synthetic air, 5 h reaction time, 8 equiv. NaOH, ratio of intended Au/HMF = 1:100).[7] The low concentration of HMF in the solution, caused by a non-optimized process for HMF synthesis, was compensated by adding commercial HMF to achieve a final HMF concentration of 0.067 M, which is comparable to other studies.[8a,9b,11b,c] This bio-derived solution modified to higher HMF concentration still contains the realistic amount of impurities, the influence of which we aim to study. We obtained a HMF conversion of 100% and a yield of 7.1% HFCA and 0% FDCA (Table 1, entry 2) with Au/ZrO_2. Under the same reaction conditions, a quantitative conversion of HMF to FDCA was obtained in pure HMF solution (0.1 M) with Au/ZrO_2 (entry 1), indicating the deactivation of the catalyst by impurities.

The formation of humins due to polymerization of HMF was a major side reaction and in order to increase FDCA yields, the formation of these by-products has to be suppressed.[18] Therefore, we addressed this issue by testing at milder reaction conditions to improve the activity of our catalyst by decreasing the rate of the formation of humins.[19] For this purpose, we changed the base from NaOH to the weaker base Na_2CO_3 and reduced the equivalents of the added base from 8 to 4. In this way, we could increase the FDCA yield to just 2.3%; however, the C-balance was enhanced to 41.1% (entry 3). Note that only HMF and its oxidation products (HFCA, DFF, FFCA, and FDCA) were taken into account for the calculation of the presented C-balance. This illustrates the considerable influence of the base and pH of the solution on the degradation of HMF to side products in presence of impurities of the chicory root-derived solution. Due to the increase in the C-balance by decreasing the alkalinity of the solution, we examined even milder conditions (100 °C, 10 bar synthetic air, and 2 equiv. Na_2CO_3; entry 4). Surprisingly, we could not observe a further increase in the C-balance under these reaction conditions with the Au/ZrO_2 catalyst.

Table 1. Screening of reaction conditions for the oxidation of HMF (0.067 M) in chicory root-derived solution HMF Chic with Au/ZrO_2 (entry 1–4) and Pt/C ip (entries 5–8; 5 h, ratio of intended Au/Pt to HMF = 1:100; entries 1 and 5: 0.1 M pure HMF solution; entry 8: after 5 h addition of another 2 equiv. Na_2CO_3 and continuation for 17 h).

Entry	Base equiv.	T [°C]	p [bar]	X(HMF) [%]	Y(HFCA) [%]	Y(FDCA) [%]	C-balance [%]
1[a]	8	125	30	>99	0	>99	>99
2[a]	8	125	30	>99	7.1	0	7.1
3[b]	4	125	30	>99	38.8	2.3	41.1
4[b]	2	100	10	76.3	27.6	0	36.2
5[b]	4	125	30	>99	0.3	81.7	82.0
6[b]	4	125	30	>99	11.8	13.8	25.6
7[b]	2	100	10	96.2	86.6	2.4	92.6
8[b]	2	100	30	>99	17.2	58.1	75.3

[a] NaOH. [b] Na2CO_3.

Next, we tested the oxidation of HMF in the bio-derived solution with Pt/C ip (impregnated) catalyst to compare the degree of deactivation for Pt. While a lower C-balance (25.6%; entry 6) was observed for Pt/C ip with 4 equiv. Na_2CO_3, the FDCA yield increased to 13.8%. Under milder conditions, Pt/C ip showed a further increase of the C-balance to 92.6% (entry 7). A simultaneous decrease in the FDCA yield was expected, mainly due to the decrease in dissolved oxygen at lower air pressure, which has a considerable influence on the FDCA yield.[8a,b] Nevertheless, Pt/C ip was more tolerant to the impurities adsorbing on the catalyst surface, making it more promising for high FDCA yields. These findings show that the noble metal used for the oxidation process has to be optimized for the use of bio-derived HMF solutions to increase its stability in presence of impurities. In addition, it is very important to adjust the pH of bio-derived solutions with impurities, which can adsorb strongly on the catalyst surface.

The high HFCA yields observed for Pt/C ip prompted us to test a two-step process: (1) HMF oxidation to HFCA with a yield of 94.3% with 2 equiv. Na_2CO_3 added to the solution, and (2) oxidation of this HFCA in a second step in a one-pot process

with the addition of another 2 equiv. Na_2CO_3. In this way, we could increase the FDCA yield to 58.1% (entry 8). This shows that the deactivation of the catalyst by impurities from the bio-based solution can be compensated, at least to some extent, by carefully adjusting the reaction conditions, particularly the alkalinity of the solution leading to a greener process. Therefore, we can conclude that the FDCA yield can be improved by using a one-pot two-step or semi-continuous process.

Analysis of the amino acid content

To unravel the cause of the deactivation of the catalyst in the chicory-derived HMF solution, we studied the presence of the compounds in the solution. Thereby, we found a considerable content of free amino acids, deriving from decomposition of proteins during the hydrothermal dehydration process, in addition to saccharides and acids in the solution. Amine and thiol functional groups are known to adsorb strongly on noble metal surfaces by physisorption or chemisorption leading to blockage and deactivation of active sites.[20] To further study their influence, first the concentration of free amino acids in HMF solutions produced from forced and non-forced chicory roots was determined (Table 2). A deviation in the concentration values before and after the oxidation reaction indicates decomposition of proteins leading to an increase in the concentration of some amino acids [e.g., cystine (denoted as Cys) and glutamic acid (GluA)]. Decrease in the concentration [e.g., for arginine (Arg) and aspartic acid (AspA)] is due to either side reactions of the amino acids or more likely due to adsorption on the noble metal surface. In addition, we observed substantial differences of the amino acid concentration depending on the use of forced or non-forced chicory roots as feedstock.

Among all amino acids found in the HMF solution, we chose an acidic (glutamic acid), an alkaline (arginine), and a sulfur-containing (cysteine and dimer cystine) amino acid for further testing. We used the highest concentration values found in the solution HMF Chic as benchmark to investigate the influence of the amino acids on the catalysts. It is worth mentioning here that the actual amount of amino acids in the reaction mixture after the oxidation reaction can be even higher but cannot be analyzed due to adsorption of amino acids on the surface of the catalyst. Hence, higher concentrations have to be considered in the investigations. The significant decrease of the FDCA yield obtained with the chicory root-derived solution, most likely due to poisoning, emphasizes the necessity to further investigate on their influence. In addition, the differences between the amino acid concentrations in the HMF solution obtained from different roots shows the importance of adjusting process and purification steps depending on the biomass source used in the process.

Influence of amino acids present in the solution on the catalytic performance of HMF oxidation

To investigate the influence of selected amino acids on the catalytic system, Au-, Pt-, Pd-, and Ru-based catalysts supported on carbon black Vulcan were prepared and tested in the HMF oxidation in presence of different concentrations of the amino acids starting with pure HMF solution. For glutamic acid (Figure 4), high concentrations $>1000\ \mu g\,mL^{-1}$ were necessary to observe any decrease of the FDCA yield or carbon balance for Au/C and Pt/C catalysts. Even at a concentration $>3000\ \mu g\,mL^{-1}$, the FDCA yield was approximately 80% for Au/C. In general, the catalyst deactivation due to glutamic acid was negligible since the interaction of the carboxylic acid groups with the metal surface is weak.

When arginine was used as an amino acid, results differed considerably (Figure 4). Especially for Au, there was a significant influence already at a concentration of about 19 $\mu g\,mL^{-1}$, a level which was present in the chicory root derived solution. For the other tested metals, the FDCA yield decreased steadily with increasing concentration. We assume that the strong interaction between the guanidine group and the noble metal surface leads to poisoning of the catalyst. For Au nanoparticles, a strong interaction with arginine was reported by Barbu-Tudoran et al.[21] which, in their study, was used for the self-assembly of nanoparticles. Since arginine has multiple functional groups available, it shows a high affinity to dissolve in water and can interact with other Au particles.[21] For Pt surfaces, chemisorption of amines under alkaline conditions was reported, which could only be removed under acidic conditions from the surface.[22]

Interestingly, a pronounced deactivation was observed for cysteine, which contains a functional thiol group that can lead to poisoning of noble metal particles (Figure 5). For all catalysts, the FDCA yield decreased to below 30% at a maximum cysteine concentration of about 50 $\mu g\,mL^{-1}$. For the adsorption of cysteine, the chemisorption via covalent bond with the Au

Table 2. Comparison of amino acid content in HMF solutions derived from forced and non-forced chicory roots.

HMF solution	Amino acid content [$\mu g\,mL^{-1}$]																
	Ala	Arg	AspA	Cys	GluA	Gly	His	Ile	Leu	Lys	Met	Phe	Pro	Ser	Thr	Tyr	Val
FCR[a]	0.4	<0.1	<0.1	<0.1	2.4	0.6	0	<0.1	0	0.3	0	0	0	<0.1	<0.1	0	<0.1
NFCR[b]	5.0	115.9	46.3	0.3	19.6	3.8	3.0	9.9	3.9	4.7	0.3	4.9	27.8	17.4	10.2	2.5	8.6
HMF Chic[a]	1.2	18.8	5.7	<0.1	1.9	1.2	0.3	0.5	<0.1	0.6	<0.1	<0.1	1.2	2.2	2.2	<0.1	0.6
HMF Chic[a,c]	2.0	<0.1	4.8	0.8	83.8	1.5	<0.1	0.2	0.1	<0.1	<0.1	<0.1	0.8	<0.1	<0.1	<0.1	0.5

[a] Forced roots. [b] Non-forced roots. [c] Analyzed after use of the solution for oxidation of HMF [Au/ZrO_2 (ratio of intended Au loading to HMF = 1:100), 125 °C, 30 bar synthetic air, 5 h, in 0.53 M NaOH].

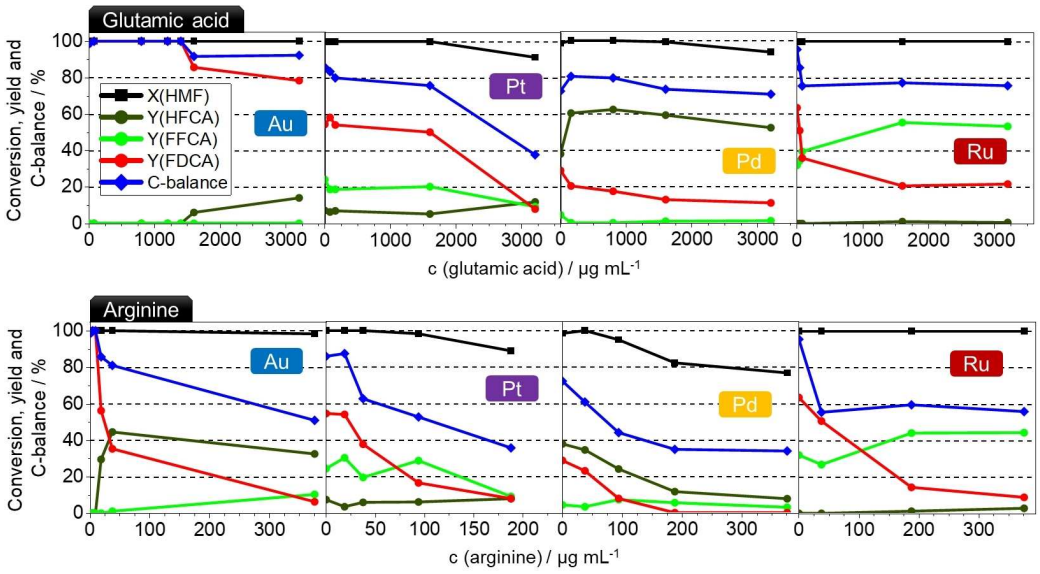

Figure 4. Influence of glutamic acid (top) and arginine (bottom) on the oxidation of HMF with Au/C, Pt/C, Pd/C, and Ru/C (100 °C, 10 bar synthetic air, 5 h, 2 equiv. Na_2CO_3, M/HMF = 1:100 or Ru/HMF = 1:50).

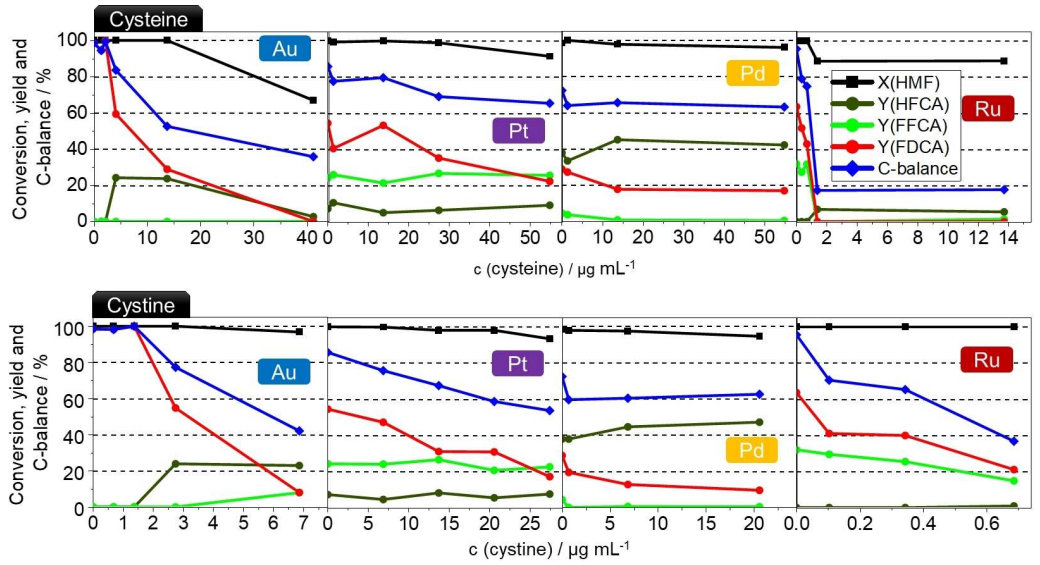

Figure 5. Influence of cysteine (top) and cystine (bottom) on the oxidation of HMF with Au/C, Pt/C, Pd/C, and Ru/C (100 °C, 10 bar synthetic air, 5 h, 2 equiv. Na_2CO_3, M/HMF = 1:100 or Ru/HMF = 1:50).

surface in a monolayer was described in an NMR study while a weakly physisorbed second layer can form on top.[20c]

Cystine was only found in very low concentrations in the HMF solution compared to other amino acids. Since it was not found in the solution before the oxidation, the actual amount could be higher due to adsorption of cystine on the catalyst surface during the reaction. Cystine showed the strongest deactivating effect of all compounds with concentrations of $< 30\ \mu g\ mL^{-1}$ being sufficient to decrease the FDCA yield to below 20% (Figure 5), probably due to a strong interaction of the sulfur with the noble metal surface by chemisorption of the functional disulfide group.

Apart from steric hindrance by the dimeric form cystine, electronic effects by polarization of the metal particle surface also play a vital role here. Furthermore, dissociation of disulfide bonds to form two covalent bonded thiol species is reported in literature.[23] This might also occur on the surface of the Au particles adsorbing cystine, which explains the roughly doubled concentration needed of the monomeric cysteine for a similar decrease in the FDCA yield. In contrast, surface-enhanced Raman scattering of cystine adsorption on Au nanoparticles displayed an intact disulfide bond and the bonding via bidentate covalent bonds of both sulfur atoms to the Au surface.[20b] Hence, the use of monometallic Au-based catalysts

for the conversion of bio-derived solutions containing such compounds should be avoided. For Pt, the binding of thiols is stronger than amines, which can show mobility on the surface as well as spillover to the support.[20a]

Improving the activity and stability with alloyed catalysts

To improve the stability and activity of noble metal-based catalysts in presence of sulfur or nitrogen-rich compounds, alloy catalysts are potential alternatives. Au and Pd were chosen for alloy formation as they showed the highest activity in pure HMF solution and a comparably stable activity in the reaction mixture, respectively. Hence, we prepared alloy catalysts with three different Au/Pd ratios to change the electronic properties of the surface like the d-electron density or d-band shape.[17a,24] In this way, we aimed at a decrease in adsorption energies of poisoning compounds, which is crucial for the use of impure bio-based solutions. The difference in the electron affinity of Au and Pd leads to an increase of s- and p-electrons for Au, while for Pd the catalytically important d-electrons increase.[25] This ultimately results in changes in the adsorbate-metal interaction. Moreover, an improved activity and stability of the oxidation state of AuPd nanoparticles by a change in d-electron density was shown by Liu et al.[17a] They could attribute the higher activity of a 25% Au containing AuPd alloy to a higher degree of surface reduction as proven by X-ray photoelectron spectroscopy (XPS) analysis. Furthermore, the rise in the activity compared to pure Pd is attributed to an Au–Pd interaction of very small Au clusters on the Pd shell observed by EXAFS fitting. A change in sulfur adsorption was reported for different alloys in literature;[26] for example, Lakhapatri and Abraham[26b] could show an increase of sulfur tolerance for a Ni-based catalyst by Rh promotion. Furthermore, Ke et al.[26a] showed an improved sulfur tolerance of a PtCo bimetallic catalyst compared to a monometallic Pt catalyst. This behavior was attributed by XPS analysis to an electron transfer from Co atoms to Pt atoms leading to a decrease of the d-band energy of Pt. This change of the electronic properties influences the interaction of sp^2-orbitals from sulfur with the Pt electrons and ultimately leads to the change in the catalyst poisoning.

All prepared AuPd alloy catalysts showed high FDCA yields ranging from 89.3 to 98.4% (see Table S2), which is comparable to the yield obtained with the monometallic Au catalyst. Further investigation of the influence of amino acids for the alloyed catalysts showed that the adsorption of arginine on the surface leads to a similar decrease in the FDCA yield as for Pd/C and Pt/C catalysts (Figure 6). The best stability against deactivation was observed for the 2:1 ratio of Au/Pd.

For the HMF oxidation in presence of cysteine, a decrease of the FDCA yield with increasing concentration was observed for all alloyed catalysts (Figure 6). Nevertheless, considerably higher concentrations of the compound can be added to the solution compared to the monometallic catalysts. Interestingly, the Au-rich catalyst AuPd(2:1)/C showed the best stability with an FDCA yield of 68.9% at a cysteine concentration of 137 $\mu g\,mL^{-1}$ although the monometallic Au catalyst was the most prone to

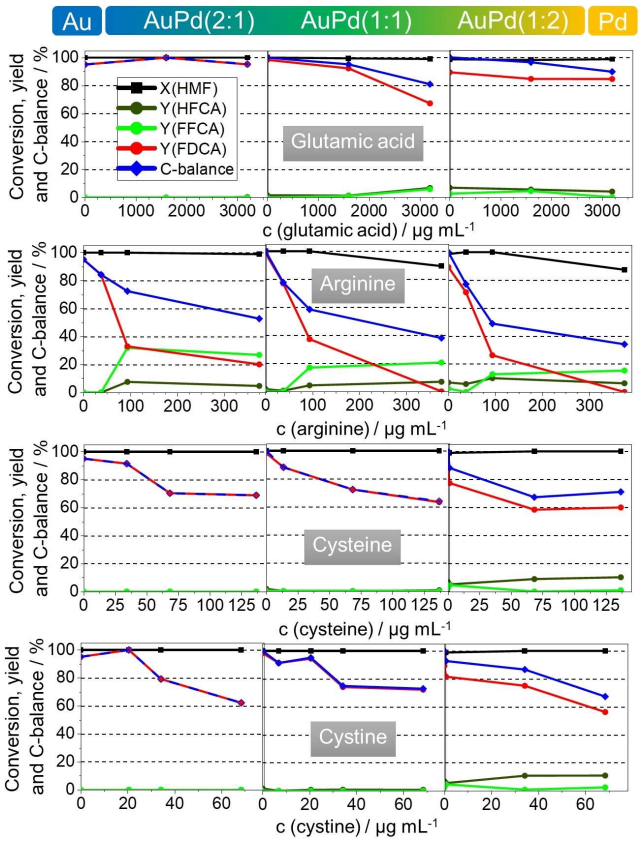

Figure 6. Influence of glutamic acid, arginine, cysteine, and cystine (from top to bottom) on the oxidation of HMF with AuPd-based catalysts (100 °C, 10 bar synthetic air, 5 h, 2 equiv. Na_2CO_3, Au + Pd/HMF = 1:100).

deactivation by cysteine. Hence, the interaction of thiols with the Au surface could be weakened by alloying with Pd and the corresponding change in the electronic properties, which influences the adsorption properties.[17a] Moreover, the presence of cystine leads to a stronger decrease of the FDCA yield. Here, the AuPd(1:1)/C catalyst showed the best stability with a FDCA yield of about 72.3% at a cystine concentration of 68.5 $\mu g\,mL^{-1}$.

To compare the influence of the tested compounds on the HMF oxidation with noble metal-based catalysts, functions were fitted to the obtained data points to calculate the concentration needed for a 10% decrease of the FDCA yield compared to the pure HMF solution (Figure 7). It can be seen that by alloying Au with Pd, a clear increase in the resistance of the catalyst against deactivation for all tested amino acids could be achieved while high yields of FDCA are maintained. Surprisingly, the concentrations of cysteine and cystine tolerated in the solution could be increased more than twofold compared to Pt/C (Figure 7). This demonstrates the applicability of a change in the electronic properties of the surface for an improved stability of catalysts for the conversion of bio-based resources. For arginine, which is the most commonly appearing amino acid in chicory root-derived solution, only a slight improvement was observed when using AuPd(2:1)/C catalyst. In this context, the arginine concentration in bio-derived HMF solution has to be monitored and, if it surpasses a critical value, it has to be regulated before

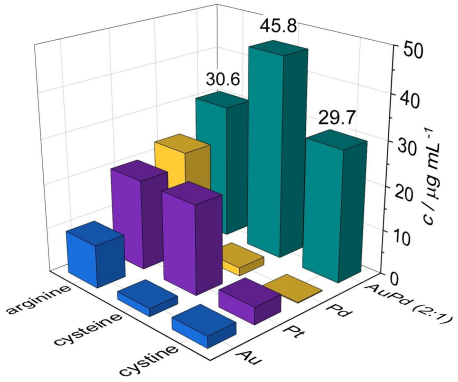

Figure 7. Concentration of amino acids needed to decrease FDCA yield by about 10% for Au/C, Pt/C, Pd/C and AuPd(2:1)/C. The concentration values of the respective amino acids for AuPd(2:1) are given in the figure (cystine: 29.7 µg mL^{-1}, cysteine: 45.8 µg mL^{-1}, arginine: 30.6 µg mL^{-1}).

performing the oxidation of HMF with noble metal based catalysts, in order to enable high FDCA yields. Moreover, AuPd(2:1)/C was tested to oxidize the chicory root-derived solution HMF Chic (125 °C, 30 bar synthetic air, 5 h, 4 equiv. Na_2CO_3, Au + Pd/HMF = 1:100) to check for the stability. Interestingly, a FDCA yield of 28.9% at quantitative HMF conversion [*Y*(HFCA) = 3.5%; *Y*(FFCA) = 11.4%] was achieved, which is a significant rise of more than twofold compared to the yield with Pt/C ip of 13.8% (FDCA yield with Au/ZrO_2: 2.3%). This unravels an improved tolerance against sulfur compounds and demonstrates the superior properties of the alloy-based catalyst.

Investigation on deactivation mechanism over alloy catalyst

The possible catalyst deactivation mechanisms upon the addition of specific amino acids to the HMF solution were investigated by considering leaching of noble metal species, particle sintering, or poisoning by strong adsorption of amino acids on the catalyst surface.[27] Firstly, we examined the stability of the catalysts with and without the addition of cysteine. Therefore, we determined the concentration of noble metal in the solution after the oxidation of HMF by ICP-OES (for details see Table S6). For AuPd(2:1)/C, neither Au nor Pd could be detected in the solution, meaning no leaching of either Au or Pd into the solution occurred, indicating the alloy composition was highly stable in the reaction medium. The degree of leaching for all catalysts was almost the same in presence of cysteine, showing that leaching was not contributing to the observed deactivation of the catalysts.

Moreover, sintering of noble metal particles influences their activity. For example, for Au/ZrO_2 and Au/C, the influence of the particle size on the activity of the catalysts was discussed in literature.[28] Naim et al.[7] observed sintering of Au particles after HMF oxidation reaction (as confirmed by powder XRD patterns), which were not visible in the as-synthesized catalyst. To investigate the role of sintering, we determined the crystallite size of nanoparticles in AuPd(2:1)/C after preparation as well as after HMF oxidation by peak fitting and using the full width at half maximum (FWHM) in the Scherrer equation (details, cf. Table S7). However, we did not observe any influence of the reaction conditions or arginine on the sintering of AuPd (2:1) nanoparticles. Hence, sintering seems to be negligible for the observed catalyst deactivation.

To further identify the role of the amino acids for the catalyst deactivation, we used ninhydrin to color different samples. Ninhydrin is used in the analysis of amino acids due to its ability to react with the primary amine function at elevated temperature by formation of so called Ruhemann's purple.[29] Due to side reactions involving the thiol function of cysteine, however, it is not possible to form Ruhemann's purple in these samples.[29] Adding ninhydrin to a solution of a blank test in HMF oxidation (100 °C, 10 bar air, 5 h, 2 equiv. Na_2CO_3, 375 µg mL^{-1} arginine) showed a change to a dark colored solution (see Figure S21). This is attributed to the reaction of ninhydrin with arginine remaining in the solution after 5 h. In addition, the formation of a shoulder at around 590 nm is observed in ultraviolet/visible spectroscopy (UV/Vis; for details see Figure S22), which is fitting to the peak by formation of Ruhemann's purple. A test with a solution produced under the same reaction conditions containing AuPd(2:1)/C catalyst did not show a color change by reaction with ninhydrin. Therefore, it can be inferred that no arginine was present anymore in the solution after 5 h. This is in agreement with the analysis performed for the experiments with chicory-based solution (see Table 2). To judge whether arginine was weakly adsorbed on the catalyst surface and can be dissolved by water or DMSO, we washed the catalyst three times with water. Afterwards ninhydrin was added to the solution and the catalyst. However, none of the samples showed a color change that can be ascribed to the reaction of arginine with ninhydrin, meaning that the amine group has been either strongly adsorbed on the catalyst surface or decomposed to other products blocking the noble metal surface and thereby leading to the poisoning of the catalyst.

Conclusion

In this study, amino acids, which are significant ingredients from proteins in biomass, were identified as considerable poison for noble metal-based catalysts during selective oxidation of 5-hydroxymethylfurfural (HMF). We propose that the strong adsorption of sulfur and the functional guanidine group on the noble metal surface leads to the deactivation of the catalysts. The identification of specific amino acids (cysteine and arginine) as critical contaminants from biomass and the estimation of their concentration limits will help to control their level and adjust purification steps for removal of these compounds, if necessary, to achieve a better suited feedstock. Consequently, the results suggest that unnecessary purification steps can be avoided if suitable conditions are used, resulting in an overall greener process chain.

Complementary to the optimization of the reaction conditions, the stability of the catalyst in presence of amino acids was significantly enhanced by alloying Pd with Au. This can be traced back to a change in the electronic and adsorption properties by alloying. Among the alloy-based catalysts, AuPd(2:1)/C showed the highest stability and activity in the presence of amino acids with 2,5-furandicarboxylic acid (FDCA) yields >90%. The improved tolerance against amino acids facilitates the reusability and long-term stability of the catalytic system, particularly promising for continuous flow applications. Furthermore, the present work leads to a better understanding of rational catalyst design for the direct use of sustainable bio-derived solutions in a bio-based chemical industry of the future. The direct conversion of more abundant agricultural by-products instead of monosaccharides to base and fine chemicals will enable us to bridge the gap from fundamental research to application and potentially open up to a more sustainable and cheaper process.

Experimental Section

Preparation of the HMF solution from chicory roots

For testing of the HMF oxidation in bio-based solution and analysis of the amino acid concentration, a HMF solution was prepared from forced chicory roots. Therefore, an extract was made from roots sliced to 4×20 mm pieces and heating them at 85±2 °C for 15 min with a ratio of biomass/water of 1:10. The extract was acidified to pH 2.5 with HNO_3 and heated to 190 °C with a residence time of 20 min in a semi-continuous reactor for HMF synthesis (denoted as HMF Chic). The solution was used after filtration with a nylon membrane filter with a pore diameter of 0.45 μm.

For comparison of amino acid concentrations, additionally, HMF solutions prepared from forced (denoted as FCR) and non-forced (NFCR) chicory roots were used. Therefore, an extract of chicory roots prepared at 85±2 °C with a ratio of biomass/water of 1:10 was used. The HMF synthesis was performed by acidification of the extract to pH 2.5 with HNO_3 and heating at 180 °C for 43 min. The solutions were used after filtration with a nylon membrane filter with a pore diameter of 0.45 μm.

Catalyst preparation

Detailed description of the catalyst preparation is given in the supporting information. An Au/ZrO_2 reference catalyst was prepared according to a deposition-precipitation procedure reported earlier by our group.[8b]

Au, Pt, and Pd-based catalysts (denoted as Au/C, Pt/C, and Pd/C) were prepared by a modified colloidal method.[12a] In brief, the respective metal chloride precursors were dissolved in water and poly(vinylalcohol) was added to the solution. Afterwards $NaBH_4$ was added to the solution, the pH was adjusted to 1 and the support was added to the formed suspension.

For the Ru catalyst (denoted as Ru/C) and Pt catalyst (denoted as Pt/C ip) an incipient-wetness impregnation was used. In brief, the metal precursor was dissolved in a mixture of 50 vol% water and 50 vol% EtOH with a total volume according to the pore volume. The solution was added dropwise under continuous mixing. Afterwards the catalyst was reduced under heating at 350 °C (Ru: 300 °C) in a 20% H_2 in N_2 mixture (3 L min^{-1}).

Procedure for the HMF oxidation

The catalytic tests were performed in stainless steel autoclaves with polytetrafluoroethylene (PTFE) inlets. 5 mL of a 0.2 M HMF solution, distilled water, and an amount of an amino acid solution according to the final concentration of the amino acid in the solution were added to yield a total volume of 10 mL. After taking a sample for measuring via HPLC, 2 equiv. of Na_2CO_3 (212 mg) and the catalyst in a ratio of M/HMF of 1:100 (only Ru: M/HMF = 1:50) were added to the solution. The pH of the solution was about 10.8 after addition of sodium carbonate. Therefore, the intended metal loading of 2 wt % was always used for the calculation. The autoclaves were purged three times with synthetic air and pressurized at the specified air pressure. Afterwards they were heated to the reaction temperature and after reaching the temperature they were stirred for 5 h. Then they were cooled down in an ice bath, depressurized, and opened. Another sample was taken and measured via HPLC for the determination of the final concentrations. For determination of the C-balance only HMF and its oxidation products HFCA, DFF, FFCA, and FDCA were taken into account as desired products.

For tests with the chicory root-derived HMF solution HMF Chic, 10.2 mL of HMF Chic, H_2O, and solid HMF were added in the same PTFE inlet to yield a total volume of 15 mL and a HMF concentration of 0.067 M. For reactions with sodium hydroxide, 2.5 M NaOH solution was added additionally to yield a total volume of 15 mL. With the addition of 2 or 4 equiv. Na_2CO_3 a pH of the solution of about 10.8 was obtained. The further procedure was as described beforehand for the use of pure HMF solution.

Acknowledgements

The authors would like to thank Veronika Holderied for assistance in HPLC analysis, Armin Lautenbach for help with ICP-OES analysis, Markus Makowiak for nitrogen physisorption measurements (BET), Roman Nickisch for fruitful discussions and Joschua Skala for the preparation of a chicory root based HMF solution. We acknowledge DESY (Hamburg, Germany), a member of the Helmholtz Association HGF, for the provision of synchrotron light, allocated in the frame of the proposal I-20200891. Parts of this research were carried out at P65 beamline at PETRA III and we would like to thank Dr. Edmund Welter for assistance in using the beamline. TEM and EDX imaging were carried out with the support of the Karlsruhe Nano Micro Facility (KNMFi, www.knmf.kit.edu), a Helmholtz Research Infrastructure at Karlsruhe Institute of Technology (KIT, www.kit.edu). TEM images and EDX-mapping were recorded by Ajai Raj Lakshmi Nilayam and Xiaohui Huang. This work was financially supported by the Federal Ministry of Food and Agriculture (BMEL) through the FNR (Fachagentur Nachwachsende Rohstoffe e. V.) based on a decision taken by the German Bundestag (funding no. 22010718). Open access funding enabled and organized by Projekt DEAL. Open Access funding enabled and organized by Projekt DEAL.

Conflict of Interest

The authors declare no conflict of interest.

Data Availability Statement

The data that support the findings of this study are available from the corresponding author upon reasonable request.

Keywords: amino acids · biomass · heterogeneous catalysis · oxidation · sustainable chemistry

[1] a) S. K. Burgess, J. E. Leisen, B. E. Kraftschik, C. R. Mubarak, R. M. Kriegel, W. J. Koros, *Macromolecules* **2014**, *47*, 1383–1391; b) A. Llevot, P.-K. Dannecker, M. von Czapiewski, L. C. Over, Z. Söyler, M. A. R. Meier, *Chem. Eur. J.* **2016**, *22*, 11510–11521; c) J. J. Bozell, G. R. Petersen, *Green Chem.* **2010**, *12*, 539–554.
[2] a) Z. Zhang, K. Deng, *ACS Catal.* **2015**, *5*, 6529–6544; b) A. D. K. Deshan, L. Atanda, L. Moghaddam, D. W. Rackemann, J. Beltramini, W. O. S. Doherty, *Front. Chem.* **2020**, *8*, 1–23.
[3] a) S. E. Davis, B. N. Zope, R. J. Davis, *Green Chem.* **2012**, *14*, 143–147; b) S. E. Davis, A. D. Benavidez, R. W. Gosselink, J. H. Bitter, K. P. de Jong, A. K. Datye, R. J. Davis, *J. Mol. Catal. A* **2014**, *388–389*, 123–132.
[4] L. Ardemani, G. Cibin, A. J. Dent, M. A. Isaacs, G. Kyriakou, A. F. Lee, C. M. A. Parlett, S. A. Parry, K. Wilson, *Chem. Sci.* **2015**, *6*, 4940–4945.
[5] a) K. Stökle, A. Kruse, *Biomass Conv. Bioref.* **2019**, *9*, 699–708; b) S. Dutta, S. De, B. Saha, *Biomass Bioenergy* **2013**, *55*, 355–369; c) N. A. S. Ramli, N. A. S. Amin, *BioEnergy Res.* **2020**, *13*, 693–736; d) T. Kläusli, *Green Process. Synth.* **2014**, *3*, 235–236; e) L. Zhu, X. Fu, Y. Hu, C. Hu, *ChemSusChem* **2020**, *13*, 4812–4832; f) Y. Román-Leshkov, J. A. Dumesic, *Top. Catal.* **2009**, *52*, 297–303.
[6] a) K. Stökle, D. Jung, A. Kruse, *Biomass Conv. Bioref.* **2020**; b) K. Stökle, B. Hülsemann, D. Steinbach, Z. Cao, H. Oechsner, A. Kruse, *Biomass Conv. Bioref.* **2021**, *11*, 1453–1463.
[7] W. Naim, O. R. Schade, E. Saraçi, D. Wüst, A. Kruse, J.-D. Grunwaldt, *ACS Sustainable Chem. Eng.* **2020**, *8*, 11512–11521.
[8] a) O. Casanova, S. Iborra, A. Corma, *ChemSusChem* **2009**, *2*, 1138–1144; b) O. R. Schade, K. F. Kalz, D. Neukum, W. Kleist, J.-D. Grunwaldt, *Green Chem.* **2018**, *20*, 3530–3541; c) S. E. Davis, L. R. Houk, E. C. Tamargo, A. K. Datye, R. J. Davis, *Catal. Today* **2011**, *160*, 55–60; d) J. Cai, H. Ma, J. Zhang, Q. Song, Z. Du, Y. Huang, J. Xu, *Chem. Eur. J.* **2013**, *19*, 14215–14223; e) N. K. Gupta, S. Nishimura, A. Takagaki, K. Ebitani, *Green Chem.* **2011**, *13*, 824; f) S. Albonetti, A. Lolli, V. Morandi, A. Migliori, C. Lucarelli, F. Cavani, *Appl. Catal. B* **2015**, *163*, 520–530.
[9] a) C. Zhou, W. Deng, X. Wan, Q. Zhang, Y. Yang, Y. Wang, *ChemCatChem* **2015**, *7*, 2853–2863; b) H. Ait Rass, N. Essayem, M. Besson, *Green Chem.* **2013**, *15*, 2240–2251; c) D. Bonincontro, A. Lolli, A. Storione, A. Gasparotto, B. Berti, S. Zacchini, N. Dimitratos, S. Albonetti, *Appl. Catal. A* **2019**, *588*, 117279; d) A. H. Motagamwala, W. Won, C. Sener, D. M. Alonso, C. T. Maravelias, J. A. Dumesic, *Sci. Adv.* **2018**, *4*, 9722.
[10] Z. Zhang, J. Zhen, B. Liu, K. Lv, K. Deng, *Green Chem.* **2015**, *17*, 1308–1317.
[11] a) G. Yi, S. P. Teong, Y. Zhang, *Green Chem.* **2016**, *18*, 979–983; b) J. Artz, R. Palkovits, *ChemSusChem* **2015**, *8*, 3832–3838; c) Y. Y. Gorbanev, S. Kegnæs, A. Riisager, *Top. Catal.* **2011**, *54*, 1318.
[12] a) A. Villa, M. Schiavoni, S. Campisi, G. M. Veith, L. Prati, *ChemSusChem* **2013**, *6*, 609–612; b) D. Bonincontro, A. Lolli, A. Villa, L. Prati, N. Dimitratos, G. M. Veith, L. E. Chinchilla, G. A. Botton, F. Cavani, S. Albonetti, *Green Chem.* **2019**, *21*, 4090–4099; c) Z. Gui, W. Cao, S. Saravanamurugan, A. Riisager, L. Chen, Z. Qi, *ChemCatChem* **2016**, *8*, 3636–3643; d) X. Wan, C. Zhou, J. Chen, W. Deng, Q. Zhang, Y. Yang, Y. Wang, *ACS Catal.* **2014**, *4*, 2175–2185; e) A. Lolli, S. Albonetti, L. Utili, R. Amadori, F. Ospitali, C. Lucarelli, F. Cavani, *Appl. Catal. A* **2015**, *504*, 408–419; f) S. Albonetti, T. Pasini, A. Lolli, M. Blosi, M. Piccinini, N. Dimitratos, J. A. Lopez-Sanchez, D. J. Morgan, A. F. Carley, G. J. Hutchings, F. Cavani, *Catal. Today* **2012**, *195*, 120–126; g) Z. Gao, R. Xie, G. Fan, L. Yang, F. Li, *ACS Sustainable Chem. Eng.* **2017**, *5*, 5852–5861.
[13] N. Sasirekha, P. Sangeetha, Y.-W. Chen, *J. Phys. Chem. C* **2014**, *118*, 15226–15233.
[14] Y. W. Lee, M. Kim, Z. H. Kim, S. W. Han, *J. Am. Chem. Soc.* **2009**, *131*, 17036–17037.
[15] O. R. Schade, F. Stein, S. Reichenberger, A. Gaur, E. Saraçi, S. Barcikowski, J.-D. Grunwaldt, *Adv. Synth. Catal.* **2020**, *362*, 5681–5696.
[16] B. Ravel, M. Newville, *J. Synchrotron Radiat.* **2005**, *12*, 537–541.
[17] a) F. Liu, D. Wechsler, P. Zhang, *Chem. Phys. Lett.* **2008**, *461*, 254–259; b) A. F. Lee, C. J. Baddeley, C. Hardacre, R. M. Ormerod, R. M. Lambert, G. Schmid, H. West, *J. Phys. Chem.* **1995**, *99*, 6096–6102; c) G. Tofighi, A. Gaur, D. E. Doronkin, H. Lichtenberg, W. Wang, D. Wang, G. Rinke, A. Ewinger, R. Dittmeyer, J.-D. Grunwaldt, *J. Phys. Chem. C* **2018**, *122*, 1721–1731.
[18] M. Kim, Y. Su, A. Fukuoka, E. J. M. Hensen, K. Nakajima, *Angew. Chem. Int. Ed.* **2018**, *57*, 8235–8239; *Angew. Chem.* **2018**, *130*, 8367–8371.
[19] a) K. I. Galkin, E. A. Krivodaeva, L. V. Romashov, S. S. Zalesskiy, V. V. Kachala, J. V. Burykina, V. P. Ananikov, *Angew. Chem. Int. Ed.* **2016**, *55*, 8338–8342; *Angew. Chem.* **2016**, *128*, 8478–8482; b) G. Tsilomelekis, M. J. Orella, Z. Lin, Z. Cheng, W. Zheng, V. Nikolakis, D. G. Vlachos, *Green Chem.* **2016**, *18*, 1983–1993; c) S. K. R. Patil, J. Heltzel, C. R. F. Lund, *Energy Fuels* **2012**, *26*, 5281–5293.
[20] a) L. Altmann, S. Kunz, M. Bäumer, *J. Phys. Chem. C* **2014**, *118*, 8925–8932; b) E. López-Tobar, B. Hernández, M. Ghomi, S. Sanchez-Cortes, *J. Phys. Chem. C* **2013**, *117*, 1531–1537; c) A. Abraham, A. J. Ilott, J. Miller, T. Gullion, *J. Phys. Chem. B* **2012**, *116*, 7771–7775; d) N. Wangoo, K. K. Bhasin, S. K. Mehta, C. R. Suri, *J. Colloid Interface Sci.* **2008**, *323*, 247–254.
[21] L. Barbu-Tudoran, G. Tomoaia, O. Horovitz, A. Mocanu, M. Tomoaia-Cotisel, *J. Optoelectron. Adv. Mater.* **2008**, *10*, 2293–2297.
[22] G. Horányi, *Electrochim. Acta* **1990**, *35*, 919–928.
[23] C. Vericat, M. E. Vela, G. Benitez, P. Carro, R. C. Salvarezza, *Chem. Soc. Rev.* **2010**, *39*, 1805–1834.
[24] a) G. Meitzner, J. H. Sinfelt, *Catal. Lett.* **1994**, *30*, 1–10; b) H. Xin, A. Vojvodic, J. Voss, J. K. Nørskov, F. Abild-Pedersen, *Phys. Rev. B* **2014**, *89*, 115114.
[25] F. Gao, D. W. Goodman, *Chem. Soc. Rev.* **2012**, *41*, 8009–8020.
[26] a) S. Ke, L. Qiu, W. Zhao, C. Sun, B. Cui, G. Xu, M. Dou, *ACS Appl. Mater. Interfaces* **2022**, *14*, 7768–7778; b) S. L. Lakhapatri, M. A. Abraham, *Catal. Sci. Technol.* **2013**, *3*, 2755–2760; c) J. A. Rodriguez, *Prog. Surf. Sci.* **2006**, *81*, 141–189.
[27] I. Sádaba, M. López Granados, A. Riisager, E. Taarning, *Green Chem.* **2015**, *17*, 4133–4145.
[28] a) O. Schade, P. Dolcet, A. Nefedov, X. Huang, E. Saraçi, C. Wöll, J.-D. Grunwaldt, *Catalysts* **2020**, *10*, 342; b) C. Megías-Sayago, A. Lolli, D. Bonincontro, A. Penkova, S. Albonetti, F. Cavani, J. A. Odriozola, S. Ivanova, *ChemCatChem* **2020**, *12*, 1177–1183.
[29] M. Friedman, *J. Agric. Food Chem.* **2004**, *52*, 385–406.

Manuscript received: February 25, 2022
Revised manuscript received: April 15, 2022
Accepted manuscript online: April 19, 2022
Version of record online: May 18, 2022